❏ 1696

Retinal blood vessel segmentation using multiple line operator-based methods

Randy Cahya Wihandika, Putra Pandu Adikara, Sigit Adinugroho, Yuita Arum Sari, Fitri Utaminingrum

Department of Computer Science, Brawijaya University, Malang, Indonesia

Article Info

ABSTRACT

The morphological alterations of the retinal blood vessels are important indicators that can be utilized to diagnose and track the progression of a number of disorders. Diabetic retinopathy (DR) is a condition that destroys the retina and is the major cause of visual loss caused by high blood glucose levels. One of the retinal objects impacted by DR is the blood vessel. By regularly monitoring changes in the retinal blood vessels, severe DR or even vision loss can be avoided. The condition of the blood vessel can be examined by segmenting the blood vessel area from a digital fundus image. Segmenting retinal blood vessels manually, on the other hand, is time-consuming and tedious, and especially when dealing with a high number of photographs. As a result, a system for segmenting retinal blood vessels automatically is crucial. Furthermore, methods for automatically segmenting retinal blood vessels are useful for person authentication systems based on the retina. Blood vessel segmentation can be accomplished in a number of ways. Based on the prior line operator method, an improved version of the line operator method is proposed in this paper. The proposed method demonstrates an improvement in accuracy over the previous method, with an accuracy of 94.61%.

Corresponding Author:

Randy Cahya Wihandika
Computer Vision Research Group, Department of Computer Science, Brawijaya University
Veteran St., Malang, East Java, Indonesia
Email: rendicahya@ub.ac.id

1. INTRODUCTION

A number of metabolic diseases such as hypertension and diabetes mellitus alter several objects in human retina, one of which is the blood vessels [1]. If the conditions remain, the alteration will also keep taking place over time. Thus, monitoring the patient's condition is crucial so that examination and treatment can be performed effectively to avoid the loss of vision. In fact, diabetic retinopathy is the primary cause of vision disorder working-age people in the world [2].

Monitoring retinal vessel blood vessel is done by analyzing the segmented fundus image in the form of binary images which separate the blood vessel pixels from background pixels. On the other hand, performing manual segmentation is exhausting and time-consuming, particularly when it involves large number of patients. It also demands specific expertise and skill. Besides, manual segmentation can suffer from human subjectivity where the segmentation results are different depending on the operator which can lead to ambiguity [2]. Therefore, automatic retinal blood vessel segmentation is essential for the monitoring process so that the time consumption can be significantly reduced while maintaining accurate segmentation results [3]. Automatic segmentation is advantegous for the diagnosis of numerous diseases, such as diabetic retinopathy

(DR), hypertensive retinopathy (HR), malaria retinopathy (MR), and glaucoma [4]. In addition, retinal blood vessel segmentation can be useful in a person identification system for various reasons: every eye has unique blood vessel pattern, the retina is stable in someone's lifetime, and it produces the best accuracy [5].

There exist different blood vessel segmentation methods in the literature which can be classified as supervised and unsupervised. Supervised methods works as binary classifiers which aim to classify each pixel to blood vessel or background [6]–[9]. Deep learning-based methods have also been proposed in numerous studies [10]–[15]. On the other hand, unsupervised methods work without involving supervised methods nor any training data. The techniques involve filters [2], [16], operators [4], [17]–[19], and region growing [20]–[23].

False positives have been the focus problem in several studies. A multi-scale approach is suggested to omit false positive pixels near large blood vessels [18]. A method for detecting false positive pixels around the retinal optic disks is proposed [19]. The pixels can then be excluded from the segmentation result in order to improve the segmentation accuracy. In this study, another technique to detect false positive pixels is proposed. Besides, a number of supervised and unsupervised methods are employed. The proposed method can be utilized as a post-processing step to improve the segmentation results of other blood vessel segmentation methods.

This paper is organized as follows. The methods used in this study is explained in section 2. The results of the experiment is explained and discussed in section 3. Finally, the conclusion of this research is given in section 4.

2. METHODS
2.1. Pre-processing

Due to several conditions in retinal fundus images, some pre-processing steps are necessary. It a common practice in performing retinal blood vessel segmentation to split the red, green, and blue (RGB) color channel and obtain only the green channel and then invert it [17]–[19]. As demonstrated in Figure 1(a), the green channel has higher contrast and less noise compared to the red channel Figure 1(b) and blue channel Figure 1(c). Besides, the green channel also has better contrast than the grayscale image obtained by averaging all the channels Figure 1(d).

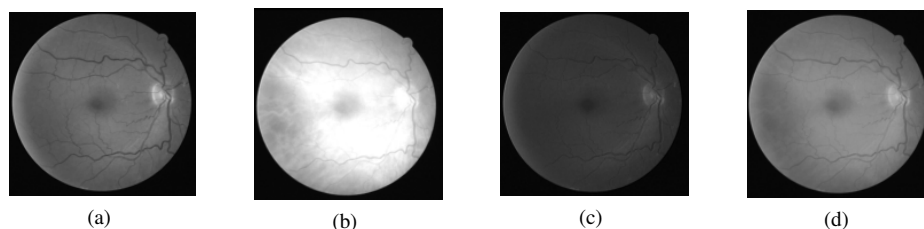(a)   (b)   (c)   (d)

Figure 1. Retinal fundus image in green channel, (b) red channel, (c) blue channel, and (d) the average of RGB channels

2.2. Line operator

The aim of the line operator method is to detect and enhance linear structures. It was first employed in [24] to detect linear structures in mammographic images then adopted in [17] to detect blood vessel in retinal fundus images. In this study, the values obtained using this method is used as one of the features for pixel classification.

The line operator's objective is to find one line which best align with the blood vessel. For example, consider an image containing one blood vessel in Figure 2. Two lines, a and b, which is of length W pixels, are put on that image which are centered at the middle of the blood vessel. Between the two lines, line a is more desired than line b since it perfectly aligns with the blood vessel. In order to choose that line, the average values are evaluated from the pixels that each line passes through. No pixel interpolation mechanism is involved in this process. Practically, the pixel coordinates can be collected using Bresenham algorithm. Then one line is selected which yields the greatest average value. Since in that image the blood vessels have higher intensity than the background, line a will result in higher average value than line b. It is because there are some parts of line b which pass through the background area while all part of line a is contained in the blood vessel.
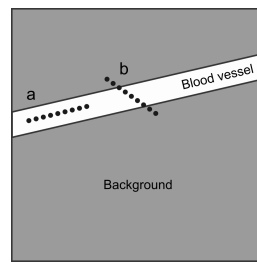
Figure 2. Line operator

To deal with blood vessels with various orientations, a number of lines with different orientations are used. The angular resolution is set to 15° so that at each pixel, 12 lines are operated, and as illustrated in Figure 3. Then the line with the highest average value I_{max}^W is chosen among those 12 lines. Moreover, the average values of the pixels located inside the window which contains the 12 lines are evaluated as well, denoted as I_{avg}^W. Lastly, I_{max}^W is subtracted from I_{avg}^W, resulting in the line strength value of the pixel, denoted as L_W:

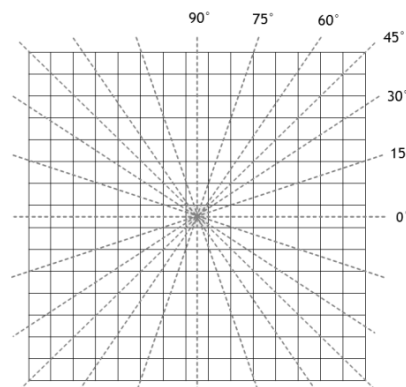$$L_W = I_{max}^W - I_{avg}^W \qquad (1)$$

Figure 3. Line orientations

As suggested in [17], the highest segmentation performance is obtained when the length of the line is set to 15 pixels. Similarly, the same length of the line is also suggested in [18] since the blood vessel width are generally 7 to 8 pixels in the digital retinal images for vessel extraction (DRIVE) dataset. Thus, the same line length is used in this study. The window, along with the 12 rotating lines, are moved to the next pixel to compute the next line strength values. In fact, the line operator method operates at every pixel in the field of view. After processing all pixels, the pixels which belong to blood vessel will have high line strength values, whereas those which belong to background will have low line strength values. That way, blood vessel pixels can be differentiated from the background. Another advantage of this method is that the uneven background intensity in the image will be more uniform.

2.3. Multi-scale line operator

The line operator explained in the previous section is able to detect and enhance linear structures of blood vessels as well as making the background intensity more even. The line strength value allows us to differentiate between blood vessels and other objects. However, it fails to perform well in some parts of retinal images. Figure 4(a) illustrate the situation located near large blood vessels. Similar situation also happen between two large blood vessels. Thresholding the image results in Figure 4(b) where a number of pixels in those areas are incorrectly recognized as vessel pixels, appearing as small blobs of pixels.

Figure 5 explains why these conditions happen when two lines, a and b are positioned near strong blood vessels. In condition a, the chosen line (i.e. the line with the highest average value) is the one which is perpendicular with the blood vessels. It is because it is the line with the most overlapping part with the blood

vessel. As a consequence, the pixels in the center of these lines result in high line strength values and thus classified as blood vessel pixels. A similar condition occurs in b where a significant part of the line overlaps with the blood vessel, resulting in strong line strength values. To overcome this misclassification problem, multiple lines with different lengths L are used in a single window of size W [18]. The L value are varied between 1 and the width of the window W ($1 \leq L \leq W$).

$$M_W^L = I_{max}^L - I_{avg}^W \tag{2}$$

(a)   (b)
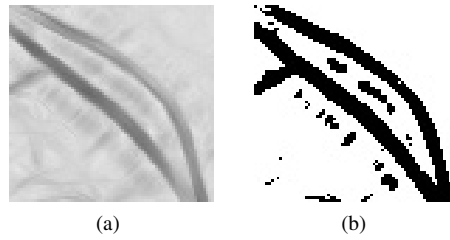
Figure 4. A drawback of the single-scale line operator (a) high response values near large blood vessels and (b) the result of thresholding image
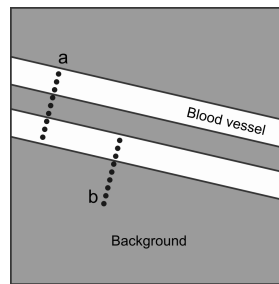

Figure 5. Situations causing false positive pixels

With different L values, each pixel will have several number of line strength values. Those values are then combined, resulting in the one single value M_{comb}:

$$M_{comb} = \frac{1}{n_L - 1} \left(\sum_L M_W^L + I_g \right) \tag{3}$$

This mechanism is able to remove false positive pixels explained previously, as demonstrated in Figure 6. This can be achieved because the combination of the line strength values is able to reduce the line strength values of the pixels located near strong blood vessels.

Figure 6. The result of the multi-scale line operator which removes false positive pixels

2.4. Optic disk segmentation

Despite the success of the multi-scale line operator, yet another false positive problem occurs in some parts of the retinal image, and specifically near the retinal optic disk. An optic disk is an object in the retina

where the nerves are located and connect to the brain, appearing as a bright circular blob in the fundus image. It can be seen in the right-hand side of Figure 1. Applying the line operator method to images containing these objects raises another false positive issue which can be seen in the red circle in Figure 7.

In order to deal with those false positive pixels, two points p and q are introduced which are placed perpendicularly to the "winning" line of the line operator method [19]. This is illustrated in Figure 8. The absolute difference between pixel intensities in position p and q is calculated, denoted as I_{opt}^{W}. Then it is involved in the line strength value formula:

$$O_W = I_{max}^{W} - I_{avg}^{W} - I_{opt}^{W} \tag{4}$$

Figure 7. False positive pixels occurring around retinal optic disk
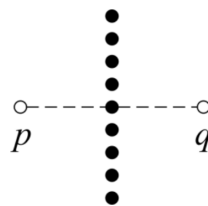

Figure 8. The position of two additional points p and q to detect optic disc pixels

The idea can be illustrated as shwon in. Consider the point located right at the edge of a retinal optic disk depicted in Figure 9. Notice that the optic disk is in low intensity and other areas outside of it is in higher intensity. Hence, the "winning" line for that point should be the one with vertical orientation since it should be the only line which does not passes through the optic disk area (i.e. the low intensity area). For that vertical line, p is positioned to the left of the line center, inside the optic disk (low intensity, and q is positioned to the right of the line center, outside the optic disk (high intensity). Therefore, the difference I_{opt}^{W} of intensity between points p and q will be high. For other areas, p and q do not have this significant difference and thus (I_{opt}^{W}) will be low. Hence, this mechanism can discriminate the pixels located at the edge of optic disks from the pixels at other areas.

This improvement is capable of detecting false positive pixels around the retinal optic disks. This image, which contains false positive pixels neighboring an optic disk, and is then subtracted from the resulting segmentation image using other methods. This will discard the false positive pixels and improves the segmentation performance. An example of this resulting image is given in Figure 10.
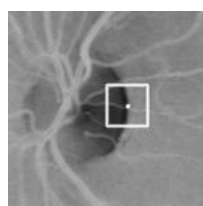

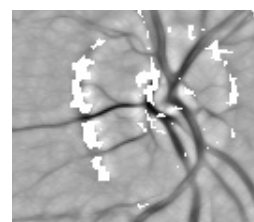Figure 9. Illustration of a situation of a point near an optic disk

Figure 10. The result of eliminating false positive pixels surrounding an optic disk

2.5. False positive detection

False positive pixels removal have been the focus of a number of studies, including this study. Specifically, the proposed method in this study focuses on the pixels near blood vessels. The aim is to obtain a new image which highlights the pixels around blood vessels. It can then be used to subtract from the resulting segmentation image using other methods to improve the segmentation result. It is achieved by modifying the line strength calculation by making it as low as possible. Recall (1) which indicates that one line with the highest line average value is chosen. The proposed method modifies this formula by choosing the line which yields the lowest line strength value I_{min}^W, instead of the highest, thus giving:

$$K_W = I_{min}^W - I_{avg}^W \tag{5}$$

The underlying idea is explained as shown in. Consider Figure 11 which shows three situations from three different points, a, b, and c. In a, the point under consideration is placed at the middle of a blood vessel. Recall the blood vessels have high intensity and other areas have low intensity. Also recall that we look for the line with the lowest line strength value I_{min}^W. Thus, lowest line strength value should be the one perpendicular to the blood vessel. It is because it has the least part which overlaps with the blood vessel. But even the lowest line strength value will still be quite high since the line has some overlapping part with the blood vessel. When (5) is applied, the resulting K_W value will be near zero because the I_{avg}^W will also be high since it contains the blood vessel.

The next point is b which is located close to the blood vessel. For that point, the line with the same orientation as the blood vessel should yield the lowest line strength value. It is because it does not cross the blood vessel at all. Hence, the lowest line strength value should be low. Since the window also include the blood vessel (same as the window in a), the K_W value should be negative.

Now consider point c which is situated in the background region with low intensity. Therefore, the $I_m^W in$ should be low for all lines in all orientations. And since the window does not contain any blood vessels, the I_{avg}^W should also be low. Hence, the K_W value should be roughly zero. This hypothesis is validated in the next section.
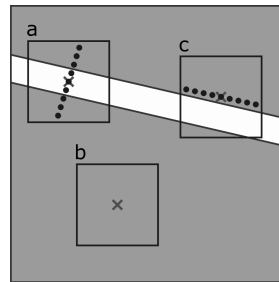

Figure 11. Three distinct situations in a fundus image

2.6. Classification

The objective of the classification in segmentation is to assign each pixel into one of the two classes, i.e. the blood vessel and the background. The features consist of i) the pre-processed green-channel intensity, ii) the single-scale line strength, and iii) the multi-scale line strength. The values in each feature are normalized prior to the classifier training process. The proposed method is applied to the resulting images from the classification. Thus, the proposed method, that aims to remove false positive pixels, can be considered as the post-processing method. Support vector machines (SVMs) with various kernels are utilized as the classification methods. For the feature, 2,000 randomly-picked pixels from the foreground (blood vessel) and background in each image are used.

3. RESULTS AND DISCUSSION

3.1. Dataset

The publicly available DRIVE dataset [25] is used in this study to measure the performance of the proposed method. The dataset contains 40 colored images which are divided into 20 train images and 20 test images. All images are acquired at the field of view of 45° using Canon CR5 non-mydriatic 3-charge-coupled

device (3-CCD) camera and are in the resolution of 565×584 pixels. All train and test images are in the color depth of 8 bits for each channel stored in TIF format. The dataset includes one binary mask image in GIF format for each train and test image which provide the field of view (FOV) of roughly 540 pixels in diameter. The white area in the mask images represent the FOV. One binary ground truth image is provided for each of the train images and two are provided for each of the test images. The ground truth images were created manually by observers. The first ground truth images are used in the experiment. The white pixels in the ground truth images denote the foreground (blood vessel).

3.2. Validation

To validate the idea of the proposed method described above, one point is taken from each condition a, b, and c. Then the I_{min}^W, I_{avg}^W and K_W values are investigated and shown in Table 1. It can be observed that the K_W value obtained from point b is negative while the value calculated from points a and c are approximately equal to zero. The values confirm the idea that it allows us to differentiate between areas near a blood vessel and other areas. Figure 12 depicts the resulting image after applying the proposed method. It can be inspected that the pixels near the blood vessels have been detected and can be used to eliminate false positive pixels.

Table 1. The value taken from three different pixels

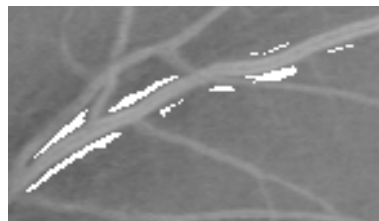| Point	I_{min}^W	I_{avg}^W	K_W
a	110	112	≈ -1
b	131	131	≈ 0
c	118	126	≈ -8

Figure 12. The result of false positive removal

3.3. Evaluation

The performance of the proposed method are evaluated in terms of accuracy, which is simply the proportion of the number of correctly classified pixels and the total number of pixels. Table 2 presents the comparison between the result of classification with and without the proposed method as the post-processing phase. The result shown in Table 2 shows that the proposed method increases the accuracy, resulting in the highest accuracy of 94.61% using the 9-degree polynomial SVM. It can also be seen that the accuracy values do not vary significantly after the proposed method is applied. It demonstrates that the classification approach is "stable" as it give similar results despite different classification methods. Figure 13 shows the final result of the segmentation. The image has been inverted for clarity.

However, there are several drawbacks of the proposed method where it fails to segment some parts of the blood vessels. Figure 14 demonstrates this situation which shows the original image, the ground truth image, and the segmentation result. The pixels located in a fine blood vessel as well as those located in the "tip" of some other vessels are ignored by the method. This occurs as a result of the thresholding step which is applied after the line operator. Pixels situated in fine blood vessels will give low line strength values. As a result, since the values are below the threshold value, they will be regarded as background pixels. Lowering the threshold value, of course, cannot be the solution since it will produce a large number of false positive pixels in other parts of the image.

Another failure is found around an optic disk, as depicted in Figure 15. In this case, the optic disk segmentation method is unsuccessful to detect the optic disk in some images. This is due to different brightness of pixels around optic disks as well as their shapes and textures across different images. This happens only in a few images which condition differs from the majority. A more careful preprocessing step and another optic disk detection approach would probably improve this condition.

Dataset quality can also lead to segmentation problems. Specifically, in some part of the dataset used in this study, the color in the edge of the retinal images appears similar to blood vessels. Even though the dataset provides mask images to mark the outer part of the retina, some mask images are not precisely positioned. Therefore, in the preprocessing, the mask images have been contracted by 10 pixels to overcome this. The line operator has also been designed not to process the outer part of the retina. However, the problem still exists in several images, which is shown in Figure 16, as false positives around the edged of the retina.

Table 2. Performance comparison

Method	Without Proposed Method	With Proposed Method
Degree-3 Polynomial SVM	87.43%	94.34%
Degree-5 Polynomial SVM	88.39%	94.44%
Degree-7 Polynomial SVM	89.67%	94.59%
Degree-9 Polynomial SVM	90.05%	94.61%
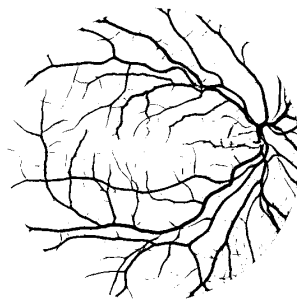
Figure 13. The final segmentation result
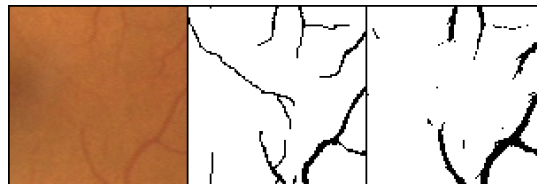
Figure 14. Segmentation failures in fine blood vessels

Figure 15. Segmentation failures around an optic disk

Figure 16. The edge of a retinal image which appearance is similar to a blood vessel

4. CONCLUSION

In this study, a retinal blood vessel segmentation method which uses classification approach and rule-based post-processing phase. Thus, it can be regarded as a combination of supervised and unsupervised techniques. The features used for the classification are formed using line operator-based methods. The unsupervised methods are used to remove false positive pixels which remain after the classification. The performance is evaluated in terms of accuracy. The highest accuracy obtained is 94.61%. However, there are a number of drawbacks found in the segmentation results, which is mainly caused by different condition of the images. Therefore, as a future work, we plan to develop a mechanism to segment fine blood vessels and also putting more work on the preprocessing to make the images more uniform in terms of brightness and color. This is because a number of segmentation failures occur due to the unequal conditions of the images in the dataset. In addition, a hemorrhage and exudate detection algorithm can also be beneficial in order to obtain better segmentation results since hemorrhages and exudates exist in some images in the dataset.

REFERENCES

[1] T. A. Soomro, *et al.*, "Impact of image enhancement technique on cnn model for retinal blood vessels segmentation," in *IEEE Access*, vol. 7, pp. 158183–158197, 2019, doi: 10.1109/ACCESS.2019.2950228.

[2] L. C. Neto, G. L. Ramalho, J. F. R. Neto, R. M. Veras, and F. N. Medeiros, "An unsupervised coarse-to-fine algorithm for blood vessel segmentation in fundus images," *Expert Systems with Applications*, vol. 78, pp. 182–192, Jul. 2017, doi: 10.1016/j.eswa.2017.02.015.

[3] M. A. Palomera-Pérez, M. E. Martinez-Perez, H. Benítez-Pérez and J. L. Ortega-Arjona, "Parallel Multiscale Feature Extraction and Region Growing: Application in Retinal Blood Vessel Detection," in *IEEE Transactions on Information Technology in Biomedicine*, vol. 14, no. 2, pp. 500–506, Mar. 2010, doi: 10.1109/TITB.2009.2036604.

[4] T. Na, J. Xie, Y. Zhao, Y. Zhao, Y. Liu, Y. Wang, and J. Liu, "Retinal vascular segmentation using superpixel-based line operator and its application to vascular topology estimation," *Medical Physics*, vol. 45, no. 7, pp. 3132–3146, May 2018, doi: 10.1002/mp.12953.

[5] M. Frucci, D. Riccio, G. S. di Baja, and L. Serino, "Severe: Segmenting vessels in retina images," *Pattern Recognition Letters*, vol. 82, pp. 162–169, Oct. 2016, doi: 10.1016/j.patrec.2015.07.002.

[6] X. Wang, X. Jiang, and J. Ren, "Blood vessel segmentation from fundus image by a cascade classification framework," *Pattern Recognition*, vol. 88, pp. 331–341, Apr. 2019, doi: 10.1016/j.patcog.2018.11.030.

[7] X. Wang and X. Jiang, "Retinal vessel segmentation by a divide-and-conquer funnel-structured classification framework," *Signal Processing*, vol. 165, pp. 104–114, Dec. 2019, doi: 10.1016/j.sigpro.2019.06.018.

[8] X.-X. Yin, S. Irshad, and Y. Zhang, "Artery/vein classification of retinal vessels using classifiers fusion," *Health Information Science and Systems*, vol. 7, no. 1, pp. 1–14, Nov. 2019, doi: 10.1007/s13755-019-0090-4.

[9] S. Aslani and H. Sarnel, "A new supervised retinal vessel segmentation method based on robust hybrid features," *Biomedical Signal Processing and Control*, vol. 30, pp. 1–12, Sep. 2016, doi: 10.1016/j.bspc.2016.05.006.

[10] K. J. Noh, S. J.Park, and S. Lee, "Scale-space approximated convolutional neural networks for retinal vessel segmentation," *Computer Methods and Programs in Biomedicine*, vol. 178, pp. 237–246, Sept. 2019, doi: 10.1016/j.cmpb.2019.06.030.

[11] S. Guo, K. Wang, H. Kang, Y. Zhang, Y. Gao, and T. Li, "Bts-dsn: Deeply supervised neural network with short connections for retinal vessel segmentation," *International Journal of Medical Informatics*, vol. 126, pp. 105–113, Jun. 2019, doi: 10.1016/j.ijmedinf.2019.03.015.

[12] A. Oliveira, S. Pereira, and C. A. Silva, "Retinal vessel segmentation based on fully convolutional neural networks," *Expert Systems with Applications*, vol. 112, pp. 229–242, Dec. 2018, doi: 10.1016/j.eswa.2018.06.034.

[13] J. H. Tan, U. R. Acharya, S. V. Bhandary, K. C. Chua, and S. Sivaprasad, "Segmentation of optic disc, fovea and retinal vasculature using a single convolutional neural network," *Journal of Computational Science*, vol. 20, pp. 70–79, May 2017, doi: 10.1016/j.jocs.2017.02.006.

[14] Q. Jin, Z. Meng, T. D. Pham, Q. Chen, L. Wei, and R. Su, "Dunet: A deformable network for retinal vessel segmentation," *Knowledge-Based Systems*, vol. 178, pp. 149–162, Aug. 2019, doi: 10.1016/j.knosys.2019.04.025.

[15] S. Feng, Z. Zhuo, D. Pan, and Q. Tian, "CcNet: A cross-connected convolutional network for segmenting retinal vessels using multi-scale features," *Neurocomputing*, vol. 392, pp. 268–276, Jun. 2020, doi: 10.1016/j.neucom.2018.10.098.

[16] W. S. Oliveira, J. V. Teixeira, T. I. Ren, G. D. C. Cavalcanti, and J. Sijbers, "Unsupervised retinal vessel segmentation using combined filters," textslPLOS ONE, vol. 11, no. 2, pp. 1–21, Feb. 2016, doi: 10.1371/journal.pone.0149943.

[17] E. Ricci and R. Perfetti, "Retinal blood vessel segmentation using line operators and support vector classification," in *IEEE Transactions on Medical Imaging*, vol. 26, no. 10, pp. 1357-1365, Oct. 2007, doi: 10.1109/TMI.2007.898551.

[18] U. T. V. Nguyen, A. Bhuiyan, L. A. F. Park, and K. Ramamohanarao, "An effective retinal blood vessel segmentation method using multi-scale line detection," *Pattern Recognition*, vol. 46, no. 3, pp. 703–715, Mar. 2013, doi: 10.1016/j.patcog.2012.08.009.

[19] R. C. Wihandika and N. Suciati, "Retinal blood vessel segmentation with optic disc pixels exclusion," *International Journal of Image, Graphics and Signal Processing*, vol. 5, no. 7, pp. 26–33, 2013, doi: 10.5815/ijigsp.2013.07.04.

[20] Y. Q. Zhao, X. H. Wang, X. F. Wang, and F. Y. Shih, "Retinal vessels segmentation based on level set and region growing," *Pattern Recognition*, vol. 47, no. 7, pp. 2437–2446, Jul. 2014, doi: 10.1016/j.patcog.2014.01.006.

[21] M. M. Almi'ani and B. D. Barkana, "A modified region growing based algorithm to vessel segmentation in magnetic resonance angiography," *2015 Long Island Systems, Applications and Technology*, 2015, pp. 1–7, doi: 10.1109/LISAT.2015.7160191.

[22] A. Bhuiyan, B. Nath, and J. J. Chua, "An adaptive region growing segmentation for blood vessel detection from retinal images," in *VISAPP*, no. 1, pp. 404–409, Mar. 2007.

[23] W. Wang, W. Wang, W. Wu, and J. Zhang, "Multi-window local region contrast adjustment and region growing for retinal vessel segmentation," in *Journal of Medical Imaging and Health Informatics*, vol. 8, no. 8, pp. 1554–1565, Oct. 2018, doi:

10.1166/jmihi.2018.2503.

[24] R. Zwiggelaar, S. M. Astley, C. R. Boggis, and C. J. Taylor, "Linear structures in mammographic images: detection and classification,," in *IEEE Transactions on Medical Imaging*,vol. 23, no. 9, pp. 1077–1086, Sep. 2004, doi: 10.1109/TMI.2004.828675.

[25] J. Staal, M. D. Abramoff, M. Niemeijer, M. A. Viergever, and B. van Ginneken, "Ridge-based vessel segmentation in color images of the retina," in *IEEE Transactions on Medical Imaging*, vol. 23, no. 4, pp. 501-509, Apr. 2004, doi: 10.1109/TMI.2004.825627.

BIOGRAPHIES OF AUTHORS

Randy Cahya Wihandika ⓘ 🇸 sc Ⓟ is a lecturer and researcher at Faculty of Computer Science, Universitas Brawijaya, Indonesia. He obtained his bachelor degree in informatics from Electronic Engineering Polytechnic Institute of Surabaya, Indonesia, in 2011. Then he pursued his master degree at Institut Teknologi Sepuluh Nopember (ITS) Indonesia, also majoring in informatics, in 2013. His interests include machine learning, image processing, and computer vision. He has published numerous publications in various journals and proceedings. He can be contacted at email: rendicahya@ub.ac.id.

Putra Pandu Adikara ⓘ 🇸 sc Ⓟ earned his bachelor degree in computer science from Faculty of Science, Brawijaya University, Indonesia, in 2007. He earned his master degree from Universitas Indonesia in 2015. His research interests are information retrieval, natural language processing, and text mining. He is currently a lecturer at the Faculty of Computer Science, Universitas Brawijaya. He can be contacted at email: adikara.putra@ub.ac.id.

Sigit Adinugroho ⓘ 🇸 sc Ⓟ got his bachelor's degree in computer science from Universitas Brawijaya, Indonesia. He earned his master's degree from Uppsala University, Sweden, majoring in Computer Science. After graduating from Uppsala University, he joined the Faculty of Computer Science, Brawijaya University, as a lecturer in the Department of Informatics. During his career as a lecturer, he has published several works in journals and conference proceeding. His main interests are machine learning, data mining, and computer vision. He also has published a book on data mining. He can be contacted at email: sigit.adinu@ub.ac.id.

Yuita Arum Sari ⓘ 🇸 sc Ⓟ received her bachelor degree at the Faculty of Mathematics and Natural Sciences, Universitas Brawijaya in 2011 and continued to master degree in the Department of Informatics, Institut Teknologi Sepuluh November, Indonesia, in 2015. She also experienced of having mobility in Computer Science, Warsaw University of Technology (non-degree program in 2014-2015). Currently, she is a lecturer in Computer Science in University of Brawijaya since 2016. She is also an active member of Laboratory of Computational Intelligence and Computer Vision Research Group. Her research area includes computer vision, image processing, machine learning, pattern recognition, and data mining. She can be contacted at email: yuita@ub.ac.id.

Fitri Utaminingrum ⓘ 🇸 sc Ⓟ was born in Surabaya, East Java, Indonesia. She is an Associate Professor at the Faculty of Computer Science, Universitas Brawijaya, Indonesia. Currently, her focus research is about the smart wheelchair, especially on the development of image algorithms. She has published her works in several reputable Scopus-indexed journals and conferences. She received her bachelor's degree in Electrical Engineering field and her master's degree in the same major from Universitas Brawijaya, Malang, Indonesia. In addition, she obtained a Doctor of Engineering in the field of computer science and electrical engineering from Kumamoto University, Japan especially focused on computer vision and image media processing. She can be contacted at email: f3ningrum@ub.ac.id.